Supplementary Information

Room-temperature electrochemical deposited polycrystalline SnO_2 with adjustable work function for high-efficiency perovskite solar cells

Yapeng Sun, Jiankai Zhang, Huangzhong Yu*

School of Physics and Optoelectronics, South China University of Technology, 510640 Guangzhou, China

*To whom correspondence should be addressed. E-mail: hzhyu@scut.edu.cn.

This PDF file includes:

Figs. S1 to S11
Tables S1 to S7

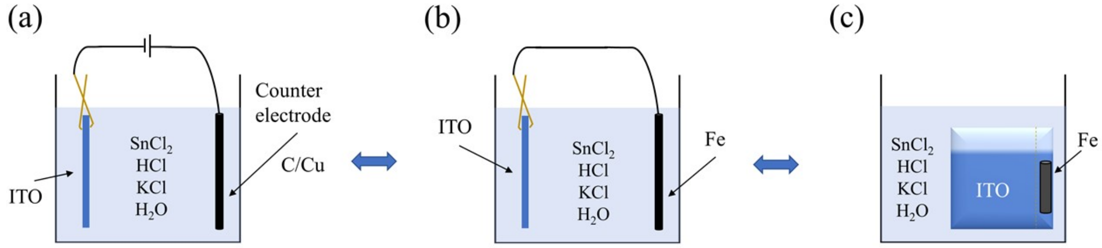

Fig. S1. (a-c) Equivalence principle schematic diagram of the deposition process.

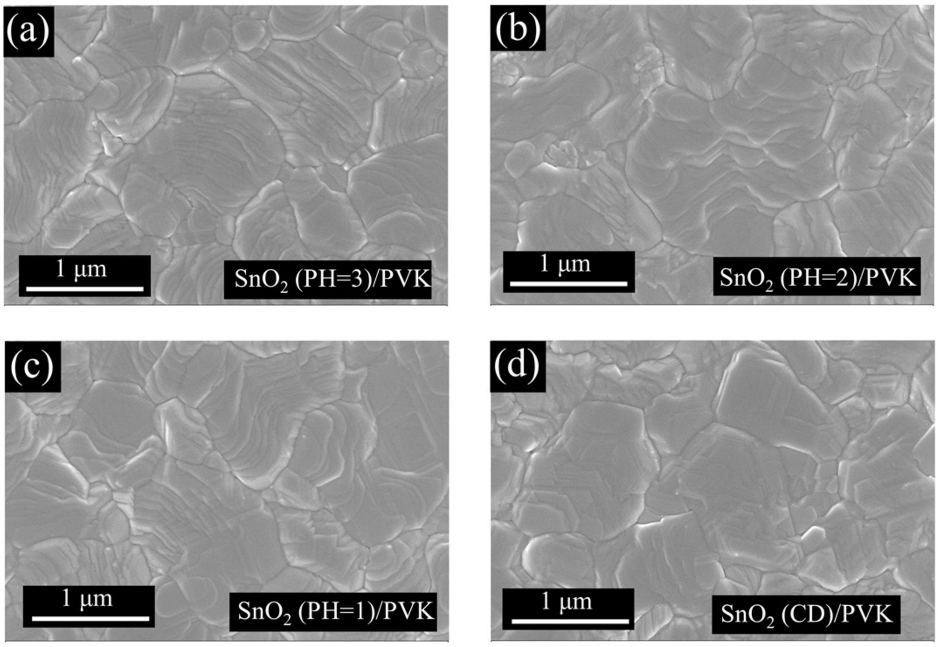

Fig. S2. (a-d) The SEM images of perovskite films on different SnO_2 films.

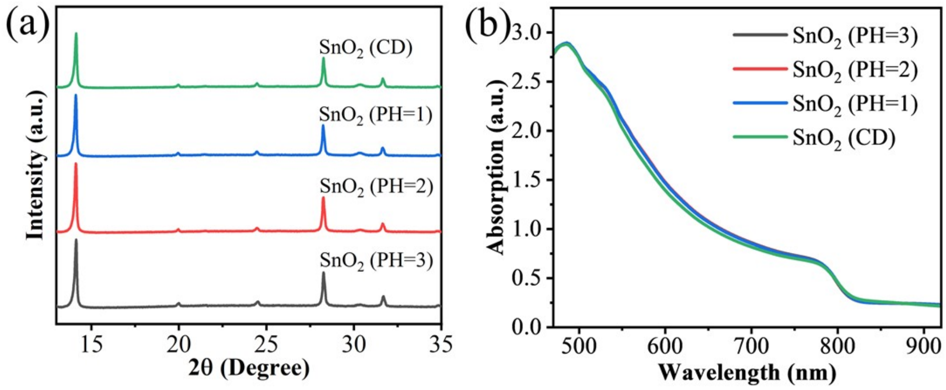

Fig. S3. (a) The XRD patterns and (b) the absorption spectrums of perovskite films on different SnO_2 films.

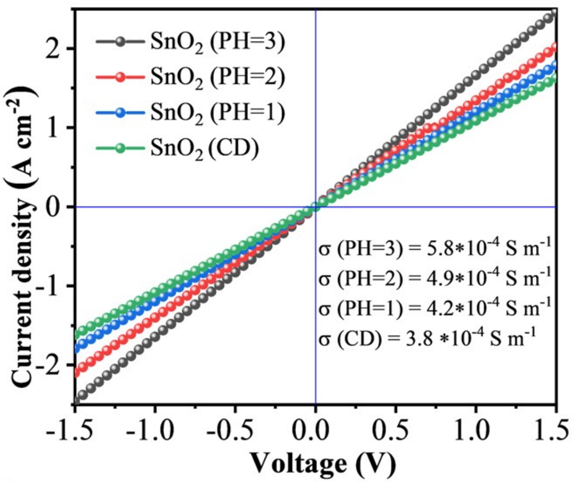

Fig. S4. The conductivity test of SnO_2 films using the *J*-*V* curves.

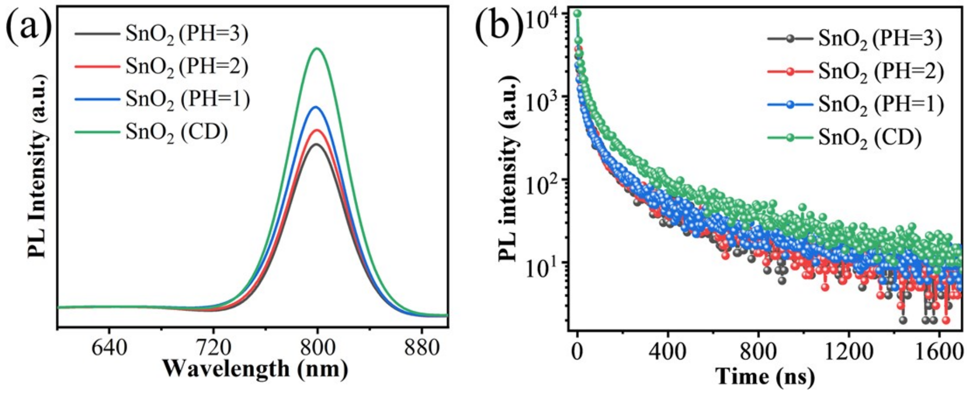

Fig. S5. (a) The PL curves and (b) the TRPL curves of perovskite films on different SnO_2 films.

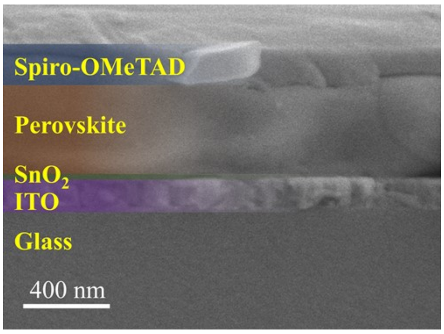

Fig. S6. The cross-sectional SEM image of device.

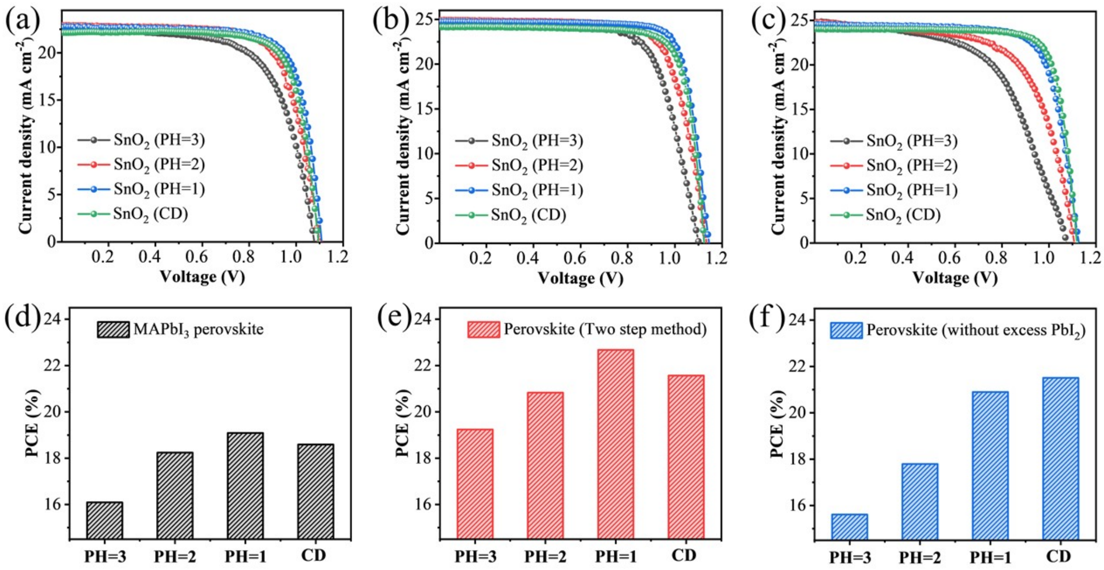

Fig. S7. (a) The reverse scanning *J-V* curves and (d) the PCE for $MAPbI_3$ devices based on different SnO_2 films. (b) The reverse scanning *J-V* curves and (e) the PCE for two-step method $(FAPbI_3)_{0.93}(MAPbI_3)_{0.07}$ perovskite devices based on different SnO_2 films. (c) The reverse scanning *J-V* curves and (f) the PCE for $FAPbI_3$ perovskite without excess PbI_2 devices based on different SnO_2 films.

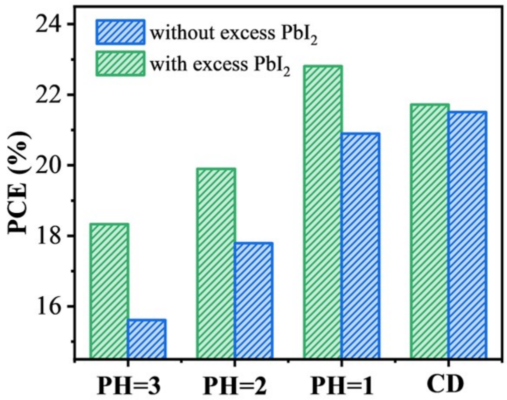

Fig. S8. The comparison figure of the device performance before and after adding excessive PbI_2 for different SnO_2 films.

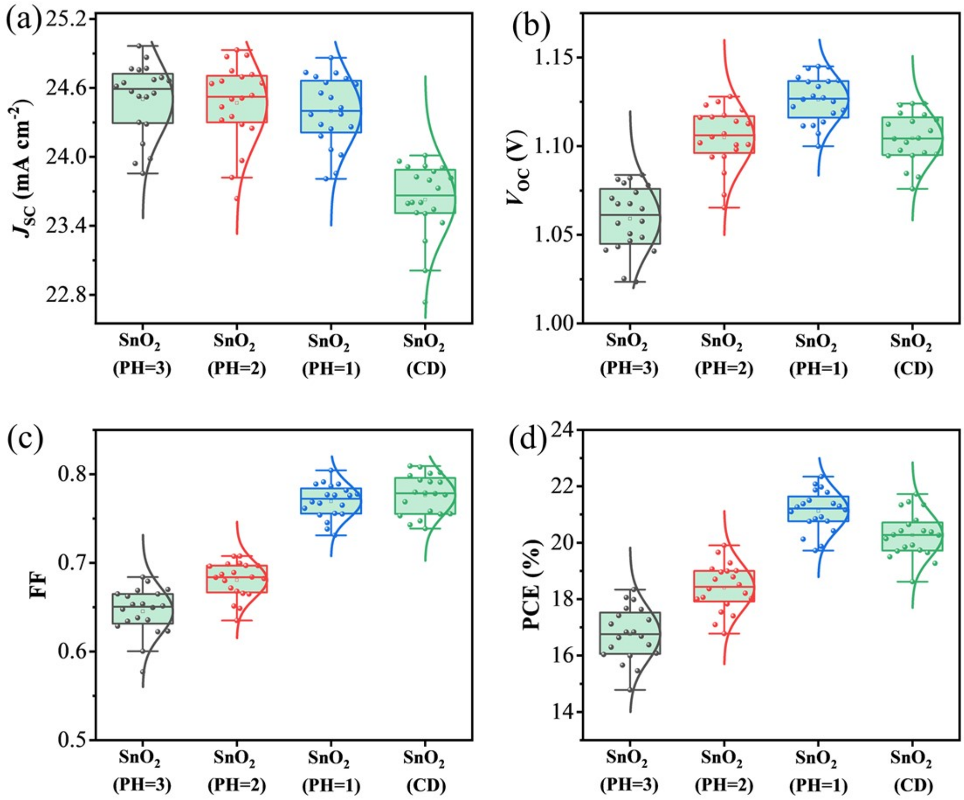

Fig. S9. (a-d) The photovoltaic parameters statistics chart for devices based on different SnO_2 films.

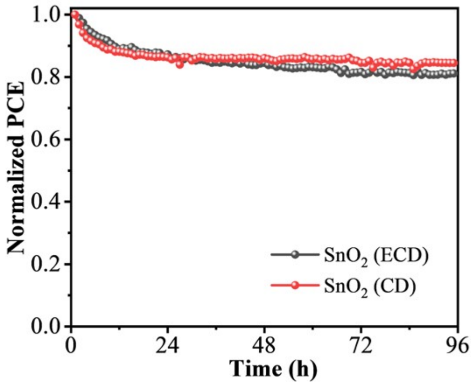

Fig. S10. Maximum power point tracking for device with different SnO_2 preparation methods measured under 1 Sun illumination without ultraviolet filter.

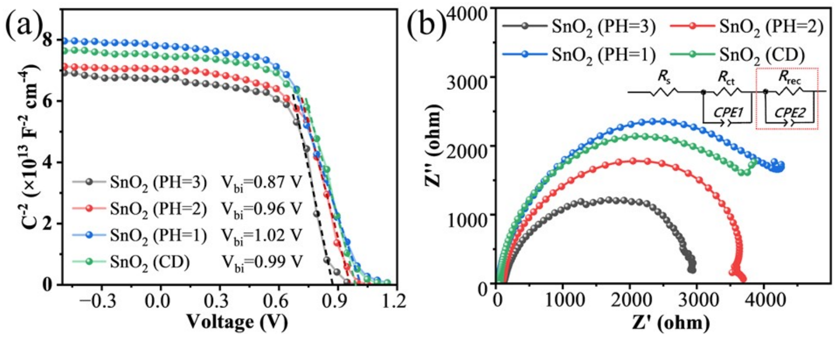

Fig. S11. (a) Mott–Schottky fitting to the C^{-2}-V curves of different devices. (b) Nyquist plots of different devices measured in the dark.

Table S1. Comparison the performance of the state-of-the-art PSCs of the low temperature prepared SnO_2 reported in the literature (PCEs denote champion values).

Preparation method	*PCE* (%)	J_{SC} (mA cm^{-2})	V_{OC} (mV)	FF (%)	Temperat -ure (°C)	Year	Ref.
Electrochemical Deposited	22.85	24.83	1144	80.44	**25**	-	This work
Commercially Colloidal Dispersion	21.72	23.92	1124	80.09	150	-	This work
Cd-SnO_2 nanocrystals	21.73	23.81	1090	84.00	90	2022	1
Mesoporous SnO_2 and RbF modification	22.72	24.50	1148	82.10	180	2021	2
Vacuum-assisted annealed SnO_2 Colloidal Dispersion	20.14	22.76	1140	77.62	100	2022	3
MXene-SnO_2 Colloidal Dispersion	19.14	24.16	1070	74.05	150	2020	4
Non-Aqueous One-Pot SnO_2 Nanoparticle Inks	18.40	21.88	1120	75.00	140	2022	5
Heterophase SnO_2 Electron Transport Bilayer	20.39	23.26	1125	77.92	190	2020	6
HEPES-Au NSs-modified SnO_2 Colloidal Dispersion	21.13	23.12	1150	79.04	150	2022	7
Zr/F Co-Doped SnO_2	19.19	24.39	1105	71.20	200	2020	8
Compact SnO_2 layer @ SnO_2 nanosheets	16.17	22.76	1050	68.00	95	2016	9
Energetically favored formation of SnO_2	19.20	22.20	1170	74.00	80	2017	10
Atomically Coherent Interlayers on	25.50	25.74	1189	83.20	190	2021	11
Chemical Bath Deposition	25.20	25.14	1181	84.80	170	2021	12
Conformal Quantum dot-SnO_2	25.39	26.28	1177	81.49	100	2022	13

Table S2. The average surface potentials of different SnO_2 films.

	SnO_2 (PH=3)	**SnO_2 (PH=2)**	**SnO_2 (PH=1)**	**SnO_2 (CD)**
KPFM (eV)	4.32	4.46	4.55	4.68

Table S3. Energy band parameters of different SnO_2 films.

	SnO_2 (PH=3)	SnO_2 (PH=2)	SnO_2 (PH=1)	SnO_2 (CD)
E_{cutoff} (eV)	16.99	16.86	16.72	16.59
W_F (eV)	4.23	4.36	4.50	4.63
E_{onset} (eV)	3.53	3.50	3.46	3.40
E_{VB} (eV)	-7.76	-7.86	-7.96	-8.03
E_{CB} (eV)	-4.13	-4.20	-4.29	-4.35

Table S4. Results of the double exponential fitting of TRPL spectra.

Sample	A_1 (%)	τ_1 (ns)	A_2 (%)	τ_2 (ns)	τ (ns)
SnO_2 (PH=3)	91.23	25.87	8.77	196.78	98.06
SnO_2 (PH=2)	93.06	27.64	6.93	231.23	105.79
SnO_2 (PH=1)	89.75	26.57	10.25	212.45	115.29
SnO_2 (CD)	88.83	37.17	11.17	251.57	135.73

Table S5. Photovoltaic performances of $MAPbI_3$ devices based on different SnO_2 films.

Material	J_{SC} (mA cm^{-2})	V_{OC} (mV)	FF (%)	PCE (%)
SnO_2 (PH=3)	22.79	1077	65.55	16.09
SnO_2 (PH=2)	22.93	1100	72.31	18.24
SnO_2 (PH=1)	22.75	1109	75.66	19.09
SnO_2 (CD)	22.16	1094	76.68	18.59

Table S6. Photovoltaic performances of two step method $(FAPb\ I_3)_{0.93}(MAPbI_3)_{0.07}$ perovskite devices based on different SnO_2 films.

Material	**J_{SC} (mA cm^{-2})**	**V_{OC} (mV)**	**FF (%)**	**PCE (%)**
SnO_2 (PH=3)	24.66	1101	70.86	19.24
SnO_2 (PH=2)	24.91	1134	73.74	20.83
SnO_2 (PH=1)	24.73	1145	80.10	22.68
SnO_2 (CD)	24.17	1124	79.40	21.57

Table S7. Photovoltaic performances of $FAPbI_3$ perovskite without excess PbI_2 devices based on different SnO_2 films.

Material	J_{SC} (mA cm^{-2})	V_{OC} (mV)	FF (%)	PCE (%)
SnO_2 (PH=3)	24.84	1074	58.51	15.61
SnO_2 (PH=2)	24.78	1108	64.79	17.79
SnO_2 (PH=1)	24.53	1128	75.53	20.90
SnO_2 (CD)	24.02	1119	80.03	21.51

References

1 J. X. Zhong, W. Q. Wu, Y. Zhou, Q. Dong, P. Wang, H. Ma, Z. Wang, C. Y. Yao, X. Chen, G. L. Liu, Y. Shi, D. B. Kuang, *Adv. Funct. Mater.*, 2022, **32**, 2200817.

2 Q. Chen, C. Peng, L. Du, T. Hou, W. Yu, D. Chen, H. Shu, D. Huang, X. Zhou, J. Zhang, W. Zhang, H. Li, J. Xie, Y. Huang, *J. Energy Chem.*, 2022, **66**, 250-259.

3 X. Li, Z. Shi, F. Behrouznejad, M. Hatamvand, X. Zhang, Y. Wang, F. Liu, H. Wang, K. Liu, H. Dong, F. Mudasar, J. Wang, A. Yu, Y. Zhan, *J. Energy Chem.*, 2022, **67**, 1-7.

4 L. Huang, X. Zhou, R. Xue, P. Xu, S. Wang, C. Xu, W. Zeng, Y. Xiong, H. Sang, D. Liang, *Nano-Micro Lett.*, 2020, **12**, 44.

5 T. a. N. Peiris, H. C. Weerasinghe, M. Sharma, J.-E. Kim, M. Michalska, N. Chandrasekaran, D. C. Senevirathna, H. Li, A. S. R. Chesman, D. Vak, J. J. Jasieniak, *Chem. Mater.*, 2022, **34**, 5535-5545.

6 H. B. Lee, N. Kumar, M. M. Ovhal, Y. J. Kim, Y. M. Song, J.-W. Kang, *Adv. Funct. Mater.*, 2020, **30**, 2001559.

7 L. Fan, P. Wang, M. Wang, W. Lü, F. Wang, H. Liu, J. Yang, L. Yang, *Chem. Eng. J.*, 2022, **427**, 131832.

8 J. Tian, J. Zhang, X. Li, B. Cheng, J. Yu, W. Ho, *Sol. RRL*, 2020, **4**, 2000090.

9 Q. Liu, M.-C. Qin, W.-J. Ke, X.-L. Zheng, Z. Chen, P.-L. Qin, L.-B. Xiong, H.-W. Lei, J.-W. Wan, J. Wen, G. Yang, J.-J. Ma, Z.-Y. Zhang, G.-J. Fang, *Adv. Funct. Mater.*, 2016, **26**, 6069-6075.

10 Q. Dong, Y. Shi, C. Zhang, Y. Wu, L. Wang, *Nano Energy*, 2017, **40**, 336-344.

11 H. Min, D. Y. Lee, J. Kim, G. Kim, K. S. Lee, J. Kim, M. J. Paik, Y. K. Kim, K. S. Kim, M. G. Kim, T. J. Shin, S. Il Seok, *Nature*, 2021, **598**, 444-450.

12 J. J. Yoo, G. Seo, M. R. Chua, T. G. Park, Y. Lu, F. Rotermund, Y. K. Kim, C. S. Moon, N. J. Jeon, J. P. Correa-Baena, V. Bulovic, S. S. Shin, M. G. Bawendi, J. Seo, *Nature*, 2021, **590**, 587-593.

13 M. Kim, J. Jeong, H. Lu, T. K. Lee, F. T. Eickemeyer, Y. Liu, I. W. Choi, S. J. Choi, Y. Jo, H. B. Kim, S. I. Mo, Y. K. Kim, H. Lee, N. G. An, S. Cho, W. R. Tress, S. M. Zakeeruddin, A. Hagfeldt, J. Y. Kim, M. Gratzel, D. S. Kim, *Science*, 2022, **375**, 302-306.